Published in final edited form as:
Brain Res. 2013 May 28; 1512: 22–36. doi:10.1016/j.brainres.2013.03.028.

Brain Axial and Radial Diffusivity Changes with Age and Gender in Healthy Adults

Rajesh Kumar[1], **Alexa S. Chavez**[1], **Paul M. Macey**[2,3], **Mary A. Woo**[2,3], and **Ronald M. Harper**[1,3,*]

[1]Department of Neurobiology, David Geffen School of Medicine at UCLA, University of California at Los Angeles, Los Angeles, CA 90095-1763, USA

[2]UCLA School of Nursing, University of California at Los Angeles, Los Angeles, CA 90095-1702, USA

[3]Brain Research Institute, University of California at Los Angeles, Los Angeles, CA 90095-1761, USA

Abstract

White matter integrity changes with age, with the extent of variation dependent on attributes such as sex and oligodendrocyte health. Quantification of myelin and axonal integrity in healthy people would provide normative values necessary to determine pathology-related tissue characteristics with normal-aging and gender. We assessed white matter integrity with diffusion tensor imaging-based axial and radial diffusivity procedures (3.0-Tesla magnetic resonance imaging), which measure water diffusion parallel and perpendicular to axonal bundles, indicating axonal and myelin status, respectively, using region-of-interest (ROI) analyses, in 34 healthy adults (age, 46.5±6.0 years, 19 male). Sex differences in diffusion values were assessed with two-sample t-tests, and diffusion changes with age using Pearson's correlations; whole-brain effect sizes were examined with voxel-based procedures. Multiple brain areas showed increased axial and radial diffusivity values reflecting declines in axonal and myelin integrity with age, especially in mid-hippocampal and posterior thalamic areas. However, axonal and myelin integrity increased in insular and occipital cortex projections with maturity. Females showed reduced fiber and myelin integrity in substantially more structures than males, and included limbic, basal ganglia, pontine, and cerebellar sites. A minority of structures, confined to cerebellar, temporal, and frontal cortices, showed reduced fiber and myelin integrity with age in males over females. Whole-brain effect sizes in diffusion values between sexes and age-related changes showed findings parallel to ROI analyses. The structural differences mandate partitioning of sex and age in adult white matter pathology assessment, and likely contribute to sex-based physiological and behavioral dysfunction in aging and in multiple pathologies.

*Corresponding Author: Ronald M. Harper, PhD, Department of Neurobiology, David Geffen School of Medicine at UCLA, University of California at Los Angeles, Los Angeles, CA 90095-1763, USA, rharper@ucla.edu, Tel: 310-825-5303, Fax: 310-825-2224.

CONFLICTS OF INTEREST: All authors have no conflicts of interest to declare.

Keywords

Magnetic resonance imaging; Diffusion tensor imaging; Myelin; Axons; Water diffusion

1. INTRODUCTION

Normal brain white matter changes occur with age in healthy adults (Ge et al., 2002; Guttmann et al., 1998), with slow degradation in fibers over time. The changes appear as loss of integrity in axons, as well as a breakdown in myelin surrounding axons (Bronge et al., 2002; Lintl and Braak, 1983; Meier-Ruge et al., 1992). The myelin breakdown may reflect underlying health of oligodendrocytes (Bartzokis, 2007), which is subject to different survival processes from axons (Funfschilling et al., 2012), and thus requires separate examination from axons in any fiber evaluation. Assessment of white matter has become increasingly important for degenerative disease appraisal, since a breakdown in fiber communication speed or integrity can lead to severe behavioral consequences (Bartzokis et al., 2010; Schiavone et al., 2009). The progression of brain tissue change differs with normal aging between sexes in several brain sites, including the thalamus, hippocampus, pontine, and parietal lobes (Kanaan et al., 2012; Menzler et al., 2011; Murphy et al., 1996; Raz et al., 2001), and these changes coincide with greater vulnerability to neuropsychological consequences between genders of similar ages (Andersen et al., 1999; Fratiglioni et al., 2000; Hammond et al., 1987; Weinshenker et al., 1989). Neural pathologies also contribute to regional white matter degradation, which can be evaluated, but only after controlling for age and sex contributions to changes in those areas, values which are largely lacking in healthy adults.

Multiple quantitative magnetic resonance imaging (MRI) procedures, including T2-relaxometry, magnetization transfer imaging (MTI), and diffusion tensor imaging (DTI) can detect white matter changes with age and sex in regional brain sites (Kumar et al., 2011a; Kumar et al., 2012b; Kumar et al., 2012c; Schiavone et al., 2009). T2-relaxometery procedures assess free water content in tissue (Loubinoux et al., 1997), in the absence of diamagnetic and paramagnetic substances, and MTI indicates myelin alterations (Engelbrecht et al., 1998), which change with normal aging and disease processes in pathological conditions. However, T2-relaxometry and MTI procedures show general tissue changes, and do not reveal specific white matter changes resulting from myelin vs. axonal impairment. Diffusion tensor imaging-based axial diffusivity measures water diffusion parallel to axons, thus revealing axonal status, and radial diffusivity assesses water diffusion perpendicular to fibers, and can assess myelin changes (Kumar et al., 2008b; Kumar et al., 2010; Kumar et al., 2011b; Song et al., 2002; Song et al., 2005). These two procedures have been used to examine fiber changes in various developmental and pathological conditions (Kumar et al., 2008b; Kumar et al., 2010; Kumar et al., 2011b; Song et al., 2002; Song et al., 2005), but such evaluation could benefit from assessment of normative values at appropriate ages, with correction for sex.

Our aim was to describe age-related myelin and axonal changes in various brain sites and sex-related differences in those areas in healthy adults using DTI-based axial and radial diffusivity procedures. We hypothesized that multiple brain areas, including the thalamus, insula, corpus callosum, and hippocampus would show age-related changes in axial and radial diffusivity values, based on changes found earlier on DTI and other MRI measures (Hasan et al., 2009; Hasan et al., 2008; Kumar et al., 2012b), and that male-female differences would also appear in the pons, thalamus, and hippocampus (Kumar et al., 2012b; Murphy et al., 1996).

2. RESULTS

2.1 Demographics

Males and females did not differ significantly by age (males vs. females; 46.6±5.0 vs. 46.3±7.3 years, $p = 0.87$). Body-mass-index showed significant differences between males and females (males vs. females; 24.9±3.2 vs. 22.4±3.9 kg/m^2, $p = 0.045$).

2.2 Brain sites with age-related changes

Multiple brain sites showed age-related changes in axial and radial diffusivity values with combined male and female data, as shown in Figure 1; whole-brain effect sizes in axial and radial diffusivity changes are also displayed (Figures 2, 3). Increased radial diffusivity emerged with advancing age in combined-sex data in left mid hippocampal fibers ($r = 0.42$, $p = 0.01$), and increased axial diffusivity appeared within axons of the bilateral posterior thalamus (left, $r = 0.50$, $p = 0.003$; right, $r = 0.38$, $p = 0.03$), and left dorsal hippocampus ($r = 0.37$, $p = 0.03$). Age-related axial diffusion changes within the left dorsal hippocampus significantly differed between males and females ($p < 0.002$). Combined male and female data, however, indicated reduced radial diffusivity, i.e., enhanced myelin status in axons within the right anterior insula ($r = -0.4$, $p = 0.02$), and decreased axial diffusivity, i.e., increased axonal integrity, within left occipital projections ($r = -0.38$, $p = 0.03$), as age increased.

Whole-brain beta maps showed an increase in axial diffusion with an increase in each unit of age (year) in most areas of the brain (Figure 2); only restricted sites in cerebellar, temporal, occipital, and frontal regions showed a decrease in axial diffusion with an increase in each unit of age, indicating preserved tissue integrity with aging. Beta maps showed an increase in radial diffusion with an increase in each unit of age, predominantly in cerebellar and deep structures in rostral brain areas (Figure 3). However, regions located closer to the surface in the rostral brain and occipital region showed a decrease in radial diffusion with an increase in each unit of age.

2.3 Male-female differences

Multiple brain sites showed significant differences in axial and radial diffusivity values between sexes (Tables 1–3); whole-brain effect size maps are presented in Figures 4 and 5. Both axial and radial diffusivity values significantly increased in females over males in the bilateral amygdala, anterior and mid thalamus, hypothalamus, superior pons, and right inferior cerebellar peduncle and putamen. Brain sites that showed significantly increased axial diffusivity included the left frontal gray matter, mid corpus callosum, right mid insula, and bilateral posterior cingulate, and increased radial diffusivity values included the right caudate nucleus, inferior pons, bilateral mid cingulate, right mid hippocampus, mid pons, and bilateral superior cerebellar peduncles in females, compared to males. However, significantly decreased axial diffusivity values emerged in the left mid cerebellar peduncle and caudal cerebellar cortex, cerebellar deep nuclei, and left inferior temporal white matter, and reduced radial diffusivity values appeared in the left frontal white matter in female compared to male subjects.

Whole-brain effect sizes in axial diffusivity between genders, derived from subtraction of averaged axial diffusivity maps of males from averaged axial diffusivity maps of females, displayed increased axial diffusion in cerebellar, temporal, and occipital sites in males compared to females (Figure 4). Other brain areas, including pontine and rostral brain sites, showed decreased axial diffusion in males over females (Figure 4). Effect sizes in radial diffusivity between sexes, derived from subtraction of averaged radial diffusivity maps of males from averaged radial diffusivity maps of females, showed increased radial diffusion in

cerebellar, frontal, and occipital regions in males compared to females (Figure 5); other sites, including pontine, thalamic, insular, and cingulate regions showed reduced effect sizes in radial diffusion in males over females (Figure 5).

3. DISCUSSION

3.1 Overview

Multiple brain areas in both male and female adults showed increased axial and radial diffusivity values with age, reflecting the expected progressive deterioration of axons and supporting myelin. The increases appeared especially in hippocampal and thalamic areas involved in memory and attention behaviors. Remarkably, selected limbic (insular cortex) and visual (occipital cortex) regions showed indices of enhanced fiber integrity, possibly reflecting better oligodendrocyte health in those areas later in life. Females showed reduced axonal and myelin integrity in substantially more structures than males, within areas ranging from limbic to basal ganglia, pontine and cerebellar sites; a minority of structures, confined to cerebellar, temporal and frontal regions, showed more fiber and myelin integrity in females. The findings mandate partitioning age- and gender-related changes during assessment of pathology-induced tissue alterations, and provide a basis for structural contributions to sex-specific vulnerabilities for neuropsychological and neuropsychiatric diseases.

3.2 Axial and radial diffusion changes with age

Brain tissue changes accompany various neurodegenerative diseases, and assessing normal structural differences are essential for evaluating pathology with aging. Age-related tissue alterations involve various subtle changes within multiple brain sites, including alterations in receptors, dendritic and spine losses, and demyelination, all of which can significantly affect synaptic transmission (Shineman et al., 2010). In many neurodegenerative diseases, pathological processes include abnormal aggregation of proteins and myelin destruction, which can lead to age-related neurocognitive deficits or neuropsychological characteristics associated with psychiatric diseases (Dickstein et al., 2007; Morrison and Hof, 1997). The non-invasive DTI-based axial and radial diffusivity procedures used here allowed examination of distinct axonal and myelin properties accompanying normal aging, and demonstrated that multiple brain regions in both males and females undergo age-related variation in both axial and radial diffusivity values. Since the greatest myelin decline with age appeared in more structures in females, a suspicion is raised that oligodendrocyte health is more compromised in females than in males, an issue of some importance for nutritional and other neuroprotective support. The enhanced myelin injury from the supportive glia is not the only concern; myelin integrity is essential for axonal survival (Funfschilling et al., 2012), and the parallel decline is of significant theoretical interest. The preferential retention of insular and occipital region myelin and axonal integrity supports the relative sparing of those central functions in vision and affect control with aging, and suggests localized glial neuroprotection.

The hippocampal findings are of interest for memory and other cognitive researchers, since increased radial diffusivity emerged with age within fibers of the mid hippocampus, suggesting myelin breakdown in a structure associated with memory as well as affective functions, and increased axial diffusivity appeared within axons of the posterior thalamus and dorsal hippocampus with age, indicating a disruption of axonal integrity. Age-related structural and functional changes in the hippocampus in normal aging have been previously noted, as reflected in brain metabolic abnormalities and volume loss (Schuff et al., 1999). Age-related volume reduction and diffusion changes have also been described by others in

normal aging in thalamic sites (Ota et al., 2007; Sullivan et al., 2004), a brain structure which is involve in visual attention (Rafal and Posner, 1987).

3.3 Male-female alterations

Differences in functional integrity of brain structures resulting from developmental morphological patterns between sexes in healthy adults can contribute to differential behavioral patterns and potential vulnerability to neuropsychological and physiological, especially cardiovascular, conditions between genders. Of all brain areas involved in neuropsychological and cardiovascular regulation, limbic structures play a major role (Drevets et al., 2008; Fuster, 2002; Oppenheimer, 2006). The white matter structural differences found here were especially apparent in limbic regions, or in brain areas with considerable influence over limbic structures, including the hypothalamus, basal-ganglia, and frontal temporal, cingulate and pontine regions. Gender differences in thalamic and hippocampal structure have been described with DTI, volumetric, and positron emission tomography based procedures. Fractional anisotropy and radial diffusivity values are reduced in males in the thalamus relative to females, findings which are parallel to our results (Menzler et al., 2011). Also, age-related volume loss in hippocampal and parietal lobes are greater in females compared to males, and metabolic consumption in thalamic and hippocampal sites are reduced in females (Murphy et al., 1996). Other brain sites, including the corpus callosum and cerebellar regions, which are important for transfer of information between limbic areas and modulation of frontal cortex action (Mittleman et al., 2008; Tan et al., 1991), respectively, emerged with axial and radial diffusivity differences between sexes.

The majority of brain sites showed either increased axial or radial diffusivity values in females over males, indicating axonal or myelin losses between genders. However, a limited number of areas showed reduced axial and radial diffusivity in females over males, suggesting that females show less pronounced axonal and myelin changes with aging in these areas, compared to similarly-aged male subjects, findings which are consistent with previous descriptions (Cowell et al., 1994; Murphy et al., 1996). These areas included sites within cerebellar, temporal, and frontal regions. Adult females perform better than males on certain cognitive tasks in later years (Seidlitz and Diener, 1998; Silverman et al., 1996), and fewer tissue changes in frontal and temporal areas in females may contribute to those cognitive advantages. Other brain sites, including pontine areas essential for regulation of breathing, pain, autonomic, and motor functions (Fenik et al., 2005; Goadsby et al., 1985; Keay et al., 1997; McGinty and Harper, 1976; Ni et al., 1990), showed more pronounced degradation of tissue in females over male subjects. Healthy adult females also show smaller pontine volumes over males (Raz et al., 2001). The collective findings are important for determining the mechanisms underlying specific pathologies associated with aging, such as the more-severe cardiovascular and neuropsychological consequences in females with obstructive sleep apnea (Macey et al., 2012; Macey et al., 2010), Alzheimer's disease (Andersen et al., 1999; Fratiglioni et al., 2000), multiple sclerosis (Hammond et al., 1987; Weinshenker et al., 1989), and heart failure.

3.4 Limitations

There are some limitations in this study, including the small number of subjects, use of a linear model to examine age-related tissue changes, normalization accuracy, unavailability of data for scanner stability and from elderly subjects, and low correlations between DTI indices and age in certain brain areas. There are also issues of interpretation of tissue changes. We found several brain sites that showed age-related tissue changes with diffusion values, and multiple brain areas with male and female differences, indicating sufficient statistical power to examine those areas. However, the small number of subjects may have precluded showing tissue changes in other brain sites because of insufficient statistical

power; some of those areas appeared in previous studies (Kanaan et al., 2012; Kumar et al., 2012b; Murphy et al., 1996). Although we had a limited number of healthy controls, the male female ratio within subjects was nearly 1:1. We used a linear model to assess age-related axial and radial diffusion changes; other studies suggest use of a curvilinear model to examine such changes (Hasan et al., 2009; Hasan et al., 2008). We believe that if pediatric and adult healthy controls composed the sample, a curvilinear model would be a more appropriate choice, but if only pediatric or only adult subjects are used, a linear model deviates little from a curvilinear model. Regional axial and radial diffusivity values were calculated from normalized axial and radial diffusivity maps using a set of region-of-interest (ROI) masks, which can affect these values for small brain sites due to interpolation in the normalization procedures. However, the normalization of diffusion maps was adequate in all subjects, and we expect little variation across subjects. On the other hand, values from smaller brain areas surrounded by fluid, including the hypothalamus, may be less reliable due to normalization errors from the partial volume effect. Although scanner stability data are not available, long-term magnetic field fluctuations can be ignored, since data acquisition was accomplished over a short time period. The high incidence of pathology in elderly subjects precluded examination of brain changes in that age group. Although axial and radial diffusivity procedures are intended principally for white matter assessment, some cortical brain sites showed axial and radial diffusion changes. Axial and radial diffusivity changes in gray matter can be interpreted as loss of tissue integrity in those sites (loss of cell alignment), and we cannot interpret those findings with respect to axons or myelin loss. Such directional measures are useful for evaluating membrane wall and leptomeningeal cortical and subcortical white matter sites (Trivedi et al., 2009; Yadav et al., 2009). Although significant, the correlations between axial and radial diffusivity values of certain brain regions and age were low, an issue that should be considered in interpretation.

3.5 Conclusions

Age and sex contribute significantly to changes in fiber structure, as assessed by axial and radial diffusivity measures in various brain areas. Sex differences appeared in multiple brain regions, including limbic, thalamic and hypothalamic sites, frontal, temporal, cingulate, and insular cortices, basal ganglia, corpus callosum, pons, and cerebellar areas. With increasing age, higher radial diffusivity emerged within mid hippocampal fibers, and increased axial diffusivity appeared within axons of the posterior thalamus and dorsal hippocampus, suggesting compromised myelin and axonal integrity, as might be expected with declining memory and other neurocognitive functions with age. However, decreased radial diffusivity appeared within axons in the anterior insula, and occipital projections relative to changes in other brain areas, suggesting that myelin integrity is maintained longer in those areas with age; such retention of central processes in affect and vision areas also confirm functional attributes that accompany normal aging. The findings demonstrate sex-based structural differences, requiring partitioning of both age and gender in white matter pathology assessment in adults. The sex-based structural changes likely contribute to gender-based differences found in both white matter structure and function found in multiple pathologies, including obstructive sleep apnea, heart failure, and Alzheimer's disease.

4. EXPERIMENTAL PROCEDURE

4.1 Subjects

Thirty-four healthy adult subjects (19 male, age 46.6±5.0 years, body-mass-index 24.9±3.2 kg/m^2, handedness, 16 right, 2 left, 1 ambidextrous; 15 female, age 46.3±7.3 years, body-mass-index 22.4±3.9 kg/m^2), handedness, 7 right, 6 left, 2 ambidextrous) were studied. All healthy control subjects were part of previously-published studies (Cross et al., 2008; Kumar et al., 2008a; Kumar et al., 2012a; Kumar et al., 2009; Kumar et al., 2011b; Macey et al.,

2008; Woo et al., 2009), and were selected for similar MRI scanning parameters, age-range, and gender ratios. We recruited all subjects through advertisements at the medical center and from the neighboring Los Angeles areas. All subjects with any neurological issues or medical conditions that might affect brain tissue were excluded from the study, as well as any subject who might not be safe in a high-magnetic field environment, as suggested by the Institute for Magnetic Resonance Safety, Education, and Research web site (http://www.mrisafety.com/). The study protocol was approved by the Institutional Review Board of the University of California at Los Angeles, and all subjects provided informed written consent prior to the study.

4.2 Magnetic resonance imaging

Brain imaging studies were performed using a 3.0-Tesla MRI scanner (Magnetom Tim-Trio; Siemens, Erlangen, Germany), with a receive-only 8-channel phased-array head-coil. We used foam pads on either side of the head to minimize head-motion during MRI data collection. High-resolution T1-weighted images were acquired using a magnetization prepared rapid acquisition gradient-echo (MPRAGE) pulse sequence [repetition-time (TR) = 2200 ms; echo-time (TE) = 2.2 ms; inversion time = 900 ms; flip angle (FA) = 9°; matrix size = 256×256; field-of-view (FOV) = 230×230 mm; slices = 176; slice thickness = 1.0 mm; slice gap = none; acquisition time = 5:25 min]. Proton-density (PD) and T2-weighted images were collected using a dual-echo turbo spin-echo pulse sequence (TR = 10,000 ms; TE1, 2 = 17, 134 ms; FA = 130°; matrix size = 256×256; FOV = 230×230 mm; turbo factor = 5; slices = ~55; slice thickness = 4.0 mm; slice gap = none; acquisition time = 4:52 min), in axial plane and covering the whole brain. Four DTI series were collected separately using a single-shot echo-planar-imaging with twice-refocused spin-echo pulse sequence (TR = 10,000 ms; TE = 87 ms; FA = 90°; bandwidth = 1346 Hz/pixel; matrix size = 128×128; FOV = 230×230 mm; slices = 77; slice thickness = 2.0 mm; slice gap = none; acquisition time = 2:40 min; diffusion gradient directions = 12; b = 0 and 700 s/mm^2). The generalized autocalibrating partially parallel acquisition (GRAPPA) parallel imaging technique, with an acceleration factor of two, was used to collect all imaging data.

4.3 Data processing

The statistical parametric mapping package SPM8 (http://www.fil.ion.ucl.ac.uk/spm/), DTI-Studio (v 3.0.1, https://www.mristudio.org/) (Jiang et al., 2006), MRIcroN (Rorden et al., 2007), and MATLAB-based (The MathWorks Inc., Natick, MA) custom software were used to process and analyze data. Proton-density- and T2-weighted images and T1-weighted images were visually-examined to confirm absence of any serious brain pathology, such as cysts, tumors, or any other lesions which may affect brain tissue diffusion values before axial and radial diffusivity calculations. No such abnormalities were present in any of these included subjects. Diffusion tensor imaging data were also examined for any motion or other imaging artifacts before data processing, and no subjects showed more than 2 mm motion between the series.

4.3.1 Axial and radial diffusivity calculation—We calculated the average background noise value from outside of the brain parenchyma with non-diffusion and diffusion-weighted images, and used this value to exclude non-brain tissue regions during axial and radial diffusivity calculation (Kumar et al., 2008b; Kumar et al., 2010; Kumar et al., 2011b). The diffusion tensor matrices were calculated using diffusion-weighted images (b = 700 s/mm^2), collected from 12 diffusion directions, and non-diffusion images (b = 0 s/mm^2), with DTI-Studio data processing software (Jiang et al., 2006). We diagonalized the diffusion tensor matrices at each voxel, and principal eigenvalues ($\lambda 1$, $\lambda 2$, and $\lambda 3$) were calculated (Basser and Pierpaoli, 1998; Pierpaoli and Basser, 1996). We used the principal eigenvalues to calculate axial ($\lambda_{||} = \lambda 1$) and radial [$\lambda_{\perp} = (\lambda 2 + \lambda 3)/2$] diffusivity maps from each DTI

series (Kumar et al., 2008b; Kumar et al., 2010; Kumar et al., 2011b; Song et al., 2002; Song et al., 2005).

4.3.2 Realignment, averaging, and normalization—Both axial and radial diffusivity maps, derived from each DTI series, were realigned to remove any potential motion between the series, and were averaged to create one axial and one radial diffusivity map for individual subjects using SPM8 software (Kumar et al., 2008b; Kumar et al., 2010; Kumar et al., 2011b). Similarly, b0 images (non-diffusion weighted images) from each series were also realigned and averaged. We normalized both averaged axial and radial diffusivity maps to Montreal Neurological Institute (MNI) space (ICBM template with European brains). For normalization, we used b0 images to partition gray, white, and cerebrospinal fluid tissue types with the unified segmentation approach (Ashburner and Friston, 2005), and the resulting normalization parameters from b0 images were applied to the corresponding axial and radial diffusivity maps and b0 images. The normalized axial and radial diffusivity maps were smoothed with a Gaussian filter (full-width-at-half-maximum, 8 mm). The normalized b0 images of all individuals were averaged to create mean background images, which were used to outline ROIs masks for regional axial and radial diffusivity analyses.

High-resolution T1-weighted images of all subjects were also normalized to MNI space, and normalized images were averaged to create background images. T1-weighted background images were used to overlay whole-brain effect size maps.

4.4 ROI analyses

We created a set of rectangular ROIs from various brain areas using mean background images, derived from normalized and averaged b0 images. These ROIs were included from gray and white matter regions of rostral, thalamic and hypothalamic, pontine, and cerebellar sites (Figure 6). All ROIs consisted of three consecutive brain slices (brain structure with maximum visibility as a middle slice, and one slice up and one slice down), with ROI sizes fitting within the examined structure for most of the brain areas. The majority of the ROIs were localized either in gray matter or in white matter, except for a few regions (e.g., thalamus) which included closely-adjacent gray and white matter, to avoid partial volume concerns. Sites were chosen from structures previously shown to be significantly affected with aging, or which showed distinctive male-female differences in particular disease processes (Cowell et al., 1994; Hasan et al., 2008; Kanaan et al., 2012; Kumar et al., 2011a; Kumar et al., 2012b; Kumar et al., 2012c; Murphy et al., 1996).

4.4.1 Rostral brain regions—Sites within the rostral brain included both gray and white matter in the amygdala, basal ganglia, and hippocampus. Bilateral regions, including the anterior, mid, and posterior cingulate and insular cortices, caudate nuclei, putamen, globus pallidus, frontal white and gray matter, amygdala, ventral, mid, and dorsal hippocampus and temporal white matter, midline occipital gray matter, and occipital white matter were examined. Unilateral areas, including the anterior, mid, and posterior corpus callosum, were also assessed.

4.4.2 Thalamic and hypothalamic areas—We examined both thalamic and hypothalamic sites. The ROIs were created within the left and right hypothalamic and thalamic regions, including anterior, mid, and posterior areas.

4.4.3 Pontine and cerebellar sites—We outlined unilateral ROIs within the pons and bilateral ROIs in cerebellar regions. Unilateral ROIs were created within the ventral, mid, caudal pons, and cerebellar deep nuclei, and bilateral ROIs were delineated within the caudal and rostral cerebellar cortices, and inferior, mid, and superior cerebellar peduncles.

4.4.4 Calculation of regional axial and radial diffusivity—We calculated average axial and radial diffusivity values from various brain sites using ROI masks and normalized axial and radial diffusivity maps, as earlier described (Kumar et al., 2011a). Regional axial and radial diffusivity values were examined for any gender differences, and also used to assess for age-related changes.

4.5 Calculation of whole-brain effect sizes

We used a linear regression model (termed "correlation with covariates" in SPM8) to examine whole-brain effect sizes in axial and radial diffusivity with age, using smoothed axial and radial diffusion maps. Beta maps, indicating changes in axial or radial diffusion values for each unit in age (year), derived from the linear models were overlaid onto background images for structural identification.

For whole-brain effect sizes between genders, smoothed axial and radial diffusivity maps from all males and females were averaged separately to create mean axial and radial maps of the two sexes. Averaged axial and radial diffusivity maps of females were subtracted from diffusion maps of males, and the corresponding subtracted maps were overlaid onto background images for structural identification.

4.6 Statistical analyses

We used the Statistical Package for the Social Sciences (SPSS V 20.0, Chicago, IL, USA) software for data analyses. Gender differences in axial and radial diffusivity values, derived from ROI analyses in different brain areas were examined with two-sample t-tests. Pearson's correlation procedures were used to assess the associations between combined male and female axial and radial diffusivity values of various brain sites with age. We considered a p value less than 0.05 statistically significant.

Acknowledgments

The authors thank Mrs. Rebecca K. Harper, Mr. Edwin M. Valladares, and Drs. Rebecca L. Cross and Stacy L. Serber for data collection assistance. This work was supported by National Institutes of Health R01 HL113251.

ABBREVIATIONS

MRI	Magnetic resonance imaging
MTI	Magnetization transfer imaging
DTI	Diffusion tensor imaging
ROI	Region-of-interest
CSF	Cerebrospinal fluid
TR	Repetition time
TE	Echo-time
FOV	Field-of-view
FA	Flip angle
MNI	Montreal Neurological Institute

References

Andersen K, Launer LJ, Dewey ME, Letenneur L, Ott A, Copeland JR, Dartigues JF, Kragh-Sorensen P, Baldereschi M, Brayne C, Lobo A, Martinez-Lage JM, Stijnen T, Hofman A. Gender differences

in the incidence of AD and vascular dementia: The EURODEM Studies. EURODEM Incidence Research Group. Neurology. 1999; 53:1992–7. [PubMed: 10599770]

Ashburner J, Friston KJ. Unified segmentation. Neuroimage. 2005; 26:839–51. [PubMed: 15955494]

Bartzokis G. Acetylcholinesterase inhibitors may improve myelin integrity. Biol Psychiatry. 2007; 62:294–301. [PubMed: 17070782]

Bartzokis G, Lu PH, Tingus K, Mendez MF, Richard A, Peters DG, Oluwadara B, Barrall KA, Finn JP, Villablanca P, Thompson PM, Mintz J. Lifespan trajectory of myelin integrity and maximum motor speed. Neurobiol Aging. 2010; 31:1554–62. [PubMed: 18926601]

Basser PJ, Pierpaoli C. A simplified method to measure the diffusion tensor from seven MR images. Magn Reson Med. 1998; 39:928–34. [PubMed: 9621916]

Bronge L, Bogdanovic N, Wahlund LO. Postmortem MRI and histopathology of white matter changes in Alzheimer brains. A quantitative, comparative study. Dement Geriatr Cogn Disorders. 2002; 13:205–12.

Cowell PE, Turetsky BI, Gur RC, Grossman RI, Shtasel DL, Gur RE. Sex differences in aging of the human frontal and temporal lobes. J Neurosci. 1994; 14:4748–55. [PubMed: 8046448]

Cross RL, Kumar R, Macey PM, Doering LV, Alger JR, Yan-Go FL, Harper RM. Neural alterations and depressive symptoms in obstructive sleep apnea patients. Sleep. 2008; 31:1103–9. [PubMed: 18714782]

Dickstein DL, Kabaso D, Rocher AB, Luebke JI, Wearne SL, Hof PR. Changes in the structural complexity of the aged brain. Aging Cell. 2007; 6:275–84. [PubMed: 17465981]

Drevets WC, Savitz J, Trimble M. The subgenual anterior cingulate cortex in mood disorders. CNS Spectr. 2008; 13:663–81. [PubMed: 18704022]

Engelbrecht V, Rassek M, Preiss S, Wald C, Modder U. Age-dependent changes in magnetization transfer contrast of white matter in the pediatric brain. Am J Neuroradiol. 1998; 19:1923–9. [PubMed: 9874548]

Fenik VB, Davies RO, Kubin L. REM sleep-like atonia of hypoglossal (XII) motoneurons is caused by loss of noradrenergic and serotonergic inputs. Am J Respir Crit Care Med. 2005; 172:1322–30. [PubMed: 16100007]

Fratiglioni L, Launer LJ, Andersen K, Breteler MM, Copeland JR, Dartigues JF, Lobo A, Martinez-Lage J, Soininen H, Hofman A. Incidence of dementia and major subtypes in Europe: A collaborative study of population-based cohorts. Neurologic Diseases in the Elderly Research Group. Neurology. 2000; 54:S10–5. [PubMed: 10854355]

Funfschilling U, Supplie LM, Mahad D, Boretius S, Saab AS, Edgar J, Brinkmann BG, Kassmann CM, Tzvetanova ID, Mobius W, Diaz F, Meijer D, Suter U, Hamprecht B, Sereda MW, Moraes CT, Frahm J, Goebbels S, Nave KA. Glycolytic oligodendrocytes maintain myelin and long-term axonal integrity. Nature. 2012; 485:517–21. [PubMed: 22622581]

Fuster JM. Frontal lobe and cognitive development. J Neurocytol. 2002; 31:373–85. [PubMed: 12815254]

Ge Y, Grossman RI, Babb JS, Rabin ML, Mannon LJ, Kolson DL. Age-related total gray matter and white matter changes in normal adult brain. Part I: volumetric MR imaging analysis. Am J Neuroradiol. 2002; 23:1327–33. [PubMed: 12223373]

Goadsby PJ, Piper RD, Lambert GA, Lance JW. Effect of stimulation of nucleus raphe dorsalis on carotid blood flow. II The cat. Am J Physiol. 1985; 248:R263–9. [PubMed: 2857529]

Guttmann CR, Jolesz FA, Kikinis R, Killiany RJ, Moss MB, Sandor T, Albert MS. White matter changes with normal aging. Neurology. 1998; 50:972–8. [PubMed: 9566381]

Hammond SR, de Wytt C, Maxwell IC, Landy PJ, English D, McLeod JG, McCall MG. The epidemiology of multiple sclerosis in Queensland, Australia. J Neurol Sci. 1987; 80:185–204. [PubMed: 3681330]

Hasan KM, Kamali A, Iftikhar A, Kramer LA, Papanicolaou AC, Fletcher JM, Ewing-Cobbs L. Diffusion tensor tractography quantification of the human corpus callosum fiber pathways across the lifespan. Brain Res. 2009; 1249:91–100. [PubMed: 18996095]

Hasan KM, Kamali A, Kramer LA, Papnicolaou AC, Fletcher JM, Ewing-Cobbs L. Diffusion tensor quantification of the human midsagittal corpus callosum subdivisions across the lifespan. Brain Res. 2008; 1227:52–67. [PubMed: 18598682]

Jiang H, van Zijl PC, Kim J, Pearlson GD, Mori S. DtiStudio: resource program for diffusion tensor computation and fiber bundle tracking. Comput Methods Programs Biomed. 2006; 81:106–16. [PubMed: 16413083]

Kanaan RA, Allin M, Picchioni M, Barker GJ, Daly E, Shergill SS, Woolley J, McGuire PK. Gender differences in white matter microstructure. PLoS One. 2012; 7:e38272. [PubMed: 22701619]

Keay KA, Crowfoot LJ, Floyd NS, Henderson LA, Christie MJ, Bandler R. Cardiovascular effects of microinjections of opioid agonists into the 'Depressor Region' of the ventrolateral periaqueductal gray region. Brain Res. 1997; 762:61–71. [PubMed: 9262159]

Kumar R, Birrer BV, Macey PM, Woo MA, Gupta RK, Yan-Go FL, Harper RM. Reduced mammillary body volume in patients with obstructive sleep apnea. Neurosci Lett. 2008a; 438:330–4. [PubMed: 18486338]

Kumar R, Chavez AS, Macey PM, Woo MA, Yan-Go FL, Harper RM. Altered global and regional brain mean diffusivity in patients with obstructive sleep apnea. J Neurosci Res. 2012a; 90:2043–52. [PubMed: 22715089]

Kumar R, Delshad S, Macey PM, Woo MA, Harper RM. Development of T2-relaxation values in regional brain sites during adolescence. Magn Reson Imaging. 2011a; 29:185–93. [PubMed: 20933351]

Kumar R, Delshad S, Woo MA, Macey PM, Harper RM. Age-related regional brain T2-relaxation changes in healthy adults. J Magn Reson Imaging. 2012b; 35:300–8. [PubMed: 21987489]

Kumar R, Macey PM, Woo MA, Alger JR, Harper RM. Diffusion tensor imaging demonstrates brainstem and cerebellar abnormalities in congenital central hypoventilation syndrome. Pediatr Res. 2008b; 64:275–80. [PubMed: 18458651]

Kumar R, Macey PM, Woo MA, Harper RM. Rostral brain axonal injury in congenital central hypoventilation syndrome. J Neurosci Res. 2010; 88:2146–54. [PubMed: 20209631]

Kumar R, Nguyen HD, Macey PM, Woo MA, Harper RM. Regional brain axial and radial diffusivity changes during development. J Neurosci Res. 2012c; 90:346–55. [PubMed: 21938736]

Kumar R, Woo MA, Birrer BV, Macey PM, Fonarow GC, Hamilton MA, Harper RM. Mammillary bodies and fornix fibers are injured in heart failure. Neurobiol Dis. 2009; 33:236–42. [PubMed: 19022386]

Kumar R, Woo MA, Macey PM, Fonarow GC, Hamilton MA, Harper RM. Brain axonal and myelin evaluation in heart failure. J Neurol Sci. 2011b; 307:106–113. [PubMed: 21612797]

Lintl P, Braak H. Loss of intracortical myelinated fibers: a distinctive age-related alteration in the human striate area. Acta Neuropathol. 1983; 61:178–82. [PubMed: 6650131]

Loubinoux I, Volk A, Borredon J, Guirimand S, Tiffon B, Seylaz J, Meric P. Spreading of vasogenic edema and cytotoxic edema assessed by quantitative diffusion and T2 magnetic resonance imaging. Stroke. 1997; 28:419–26. [PubMed: 9040700]

Macey PM, Kumar R, Woo MA, Valladares EM, Yan-Go FL, Harper RM. Brain structural changes in obstructive sleep apnea. Sleep. 2008; 31:967–77. [PubMed: 18652092]

Macey PM, Kumar R, Yan-Go FL, Woo MA, Harper RM. Sex differences in white matter alterations accompanying obstructive sleep apnea. Sleep. 2012; 35:1603–13. [PubMed: 23204603]

Macey PM, Woo MA, Kumar R, Cross RL, Harper RM. Relationship between obstructive sleep apnea severity and sleep, depression and anxiety symptoms in newly-diagnosed patients. PLoS One. 2010; 5:e10211. [PubMed: 20419135]

McGinty DJ, Harper RM. Dorsal raphe neurons: depression of firing during sleep in cats. Brain Res. 1976; 101:569–75. [PubMed: 1244990]

Meier-Ruge W, Ulrich J, Bruhlmann M, Meier E. Age-related white matter atrophy in the human brain. Ann N Y Acad Sci. 1992; 673:260–9. [PubMed: 1485724]

Menzler K, Belke M, Wehrmann E, Krakow K, Lengler U, Jansen A, Hamer HM, Oertel WH, Rosenow F, Knake S. Men and women are different: diffusion tensor imaging reveals sexual dimorphism in the microstructure of the thalamus, corpus callosum and cingulum. Neuroimage. 2011; 54:2557–62. [PubMed: 21087671]

Mittleman G, Goldowitz D, Heck DH, Blaha CD. Cerebellar modulation of frontal cortex dopamine efflux in mice: relevance to autism and schizophrenia. Synapse. 2008; 62:544–50. [PubMed: 18435424]

Morrison JH, Hof PR. Life and death of neurons in the aging brain. Science. 1997; 278:412–9. [PubMed: 9334292]

Murphy DG, DeCarli C, McIntosh AR, Daly E, Mentis MJ, Pietrini P, Szczepanik J, Schapiro MB, Grady CL, Horwitz B, Rapoport SI. Sex differences in human brain morphometry and metabolism: an in vivo quantitative magnetic resonance imaging and positron emission tomography study on the effect of aging. Arch Gen Psychiatry. 1996; 53:585–94. [PubMed: 8660125]

Ni HF, Zhang JX, Harper RM. Respiratory-related discharge of periaqueductal gray neurons during sleep-waking states. Brain Res. 1990; 511:319–25. [PubMed: 2334849]

Oppenheimer S. Cerebrogenic cardiac arrhythmias: cortical lateralization and clinical significance. Clin Auton Res. 2006; 16:6–11. [PubMed: 16477489]

Ota M, Obata T, Akine Y, Ito H, Matsumoto R, Ikehira H, Asada T, Suhara T. Laterality and aging of thalamic subregions measured by diffusion tensor imaging. Neuroreport. 2007; 18:1071–5. [PubMed: 17558299]

Pierpaoli C, Basser PJ. Toward a quantitative assessment of diffusion anisotropy. Magn Reson Med. 1996; 36:893–906. [PubMed: 8946355]

Rafal RD, Posner MI. Deficits in human visual spatial attention following thalamic lesions. Proceedings of the Natl Acad Sci U S A. 1987; 84:7349–53.

Raz N, Gunning-Dixon F, Head D, Williamson A, Acker JD. Age and sex differences in the cerebellum and the ventral pons: a prospective MR study of healthy adults. Am J Neuroradiol. 2001; 22:1161–7. [PubMed: 11415913]

Rorden C, Karnath HO, Bonilha L. Improving lesion-symptom mapping. J Cogn Neurosci. 2007; 19:1081–8. [PubMed: 17583985]

Schiavone F, Charlton RA, Barrick TR, Morris RG, Markus HS. Imaging age-related cognitive decline: A comparison of diffusion tensor and magnetization transfer MRI. J Magn Reson Imaging. 2009; 29:23–30. [PubMed: 19097099]

Schuff N, Amend DL, Knowlton R, Norman D, Fein G, Weiner MW. Age-related metabolite changes and volume loss in the hippocampus by magnetic resonance spectroscopy and imaging. Neurobiol Aging. 1999; 20:279–85. [PubMed: 10588575]

Seidlitz L, Diener E. Sex differences in the recall of affective experiences. J Pers Soc Psychol. 1998; 74:262–71. [PubMed: 9457787]

Shineman DW, Salthouse TA, Launer LJ, Hof PR, Bartzokis G, Kleiman R, Luine V, Buccafusco JJ, Small GW, Aisen PS, Lowe DA, Fillit HM. Therapeutics for cognitive aging. Ann N Y Acad Sci. 2010; 1191(Suppl 1):E1–15. [PubMed: 20392284]

Silverman I, Phillips K, Silverman LK. Homogeneity of effect sizes for sex across spatial tests and cultures: implications for hormonal theories. Brain Cogn. 1996; 31:90–4. [PubMed: 8790937]

Song SK, Sun SW, Ramsbottom MJ, Chang C, Russell J, Cross AH. Dysmyelination revealed through MRI as increased radial (but unchanged axial) diffusion of water. Neuroimage. 2002; 17:1429–36. [PubMed: 12414282]

Song SK, Yoshino J, Le TQ, Lin SJ, Sun SW, Cross AH, Armstrong RC. Demyelination increases radial diffusivity in corpus callosum of mouse brain. Neuroimage. 2005; 26:132–40. [PubMed: 15862213]

Sullivan EV, Rosenbloom M, Serventi KL, Pfefferbaum A. Effects of age and sex on volumes of the thalamus, pons, and cortex. Neurobiol Aging. 2004; 25:185–92. [PubMed: 14749136]

Tan YL, Chen BH, Yang JD, Zhang J, Wang YC, Chai SH, Wang ZY, Li QH. Localization of functional projections from corpus callosum to cerebral cortex. Chin Med J. 1991; 104:851–7. [PubMed: 1752144]

Trivedi R, Husain N, Rathore RK, Saksena S, Srivastava S, Malik GK, Das V, Pradhan M, Pandey CM, Gupta RK. Correlation of diffusion tensor imaging with histology in the developing human frontal cerebrum. Dev Neurosci. 2009; 31:487–96. [PubMed: 19622880]

Weinshenker BG, Bass B, Rice GP, Noseworthy J, Carriere W, Baskerville J, Ebers GC. The natural history of multiple sclerosis: a geographically based study. I Clinical course and disability. Brain. 1989; 112 (Pt 1):133–46. [PubMed: 2917275]

Woo MA, Kumar R, Macey PM, Fonarow GC, Harper RM. Brain injury in autonomic, emotional, and cognitive regulatory areas in patients with heart failure. J Card Fail. 2009; 15:214–23. [PubMed: 19327623]

Yadav A, Malik GK, Trivedi R, Prasad A, Nath K, Prasad KN, Agrawal P, Rathore RK, Tripathi RP, Gupta RK. Correlation of CSF neuroinflammatory molecules with leptomeningeal cortical subcortical white matter fractional anisotropy in neonatal meningitis. Magn Reson Imaging. 2009; 27:214–21. [PubMed: 18687548]

HIGHLIGHTS

- Developmental changes in myelin and axons by sex were assessed in healthy adults.
- Myelin and axonal integrity declined with age, except in insular and occipital sites.
- Integrity declines were especially marked in hippocampus and posterior thalamus.
- Females showed more axonal and myelin changes in multiple structures than males.
- The findings show the need to control age and sex in fiber assessment of mixed groups.

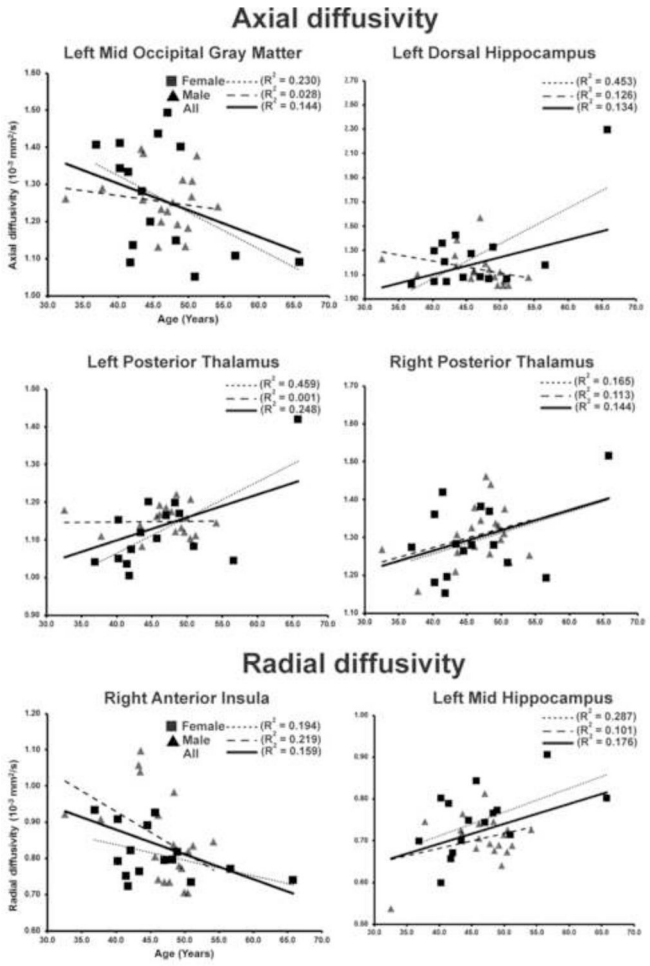

Figure 1.

Relationships between combined, and separately, male, and female axial and radial diffusivity values and age. Corresponding solid and dotted lines on the scatter plots shows best fit lines for the combined (n = 34), male (n = 19), and female (n = 15) axial and radial diffusivity data.

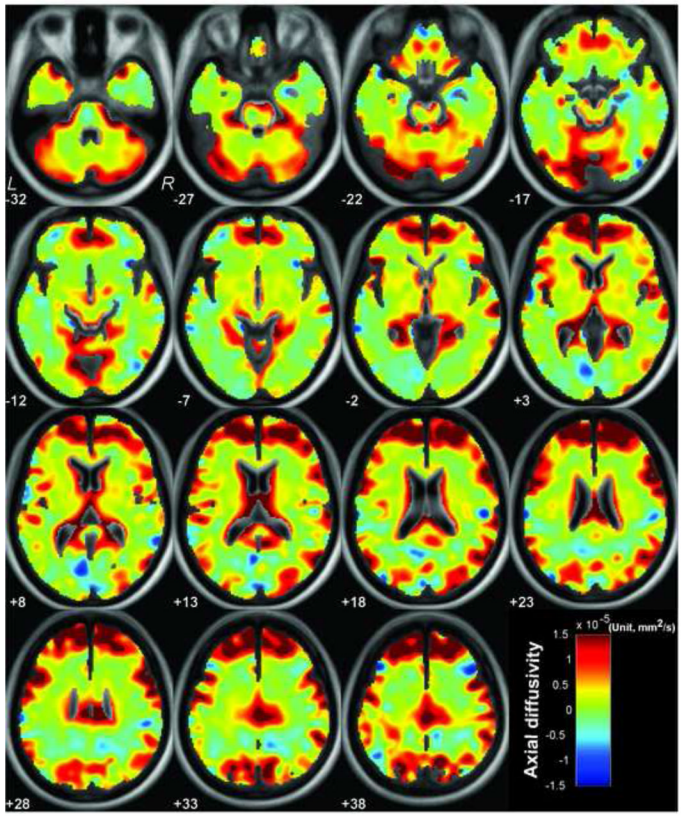

Figure 2.

Whole-brain axial diffusivity changes with per unit increase in age (year). Brain sites with increased and decreased axial diffusivity with per unit increase in age are overlaid onto T1-weighted background images. Warm colors indicate positive effect sizes between axial diffusivity and age, and cooler colors show regions with negative effect sizes between axial diffusivity and age. Maps are displayed in axial views with neurological convention (*L = Left, R = Right*), and corresponding slice locations are indicated in MNI space. Color scale shows both positive and negative axial diffusion values.

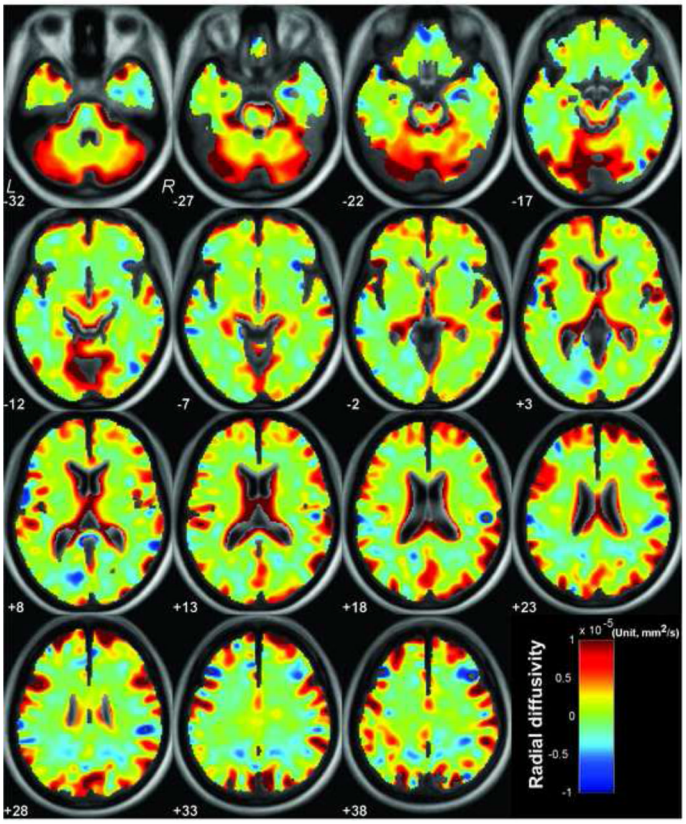

Figure 3.
Whole-brain radial diffusivity changes with unit increase in age (year). Other figure conventions are the same as in Figure 2.

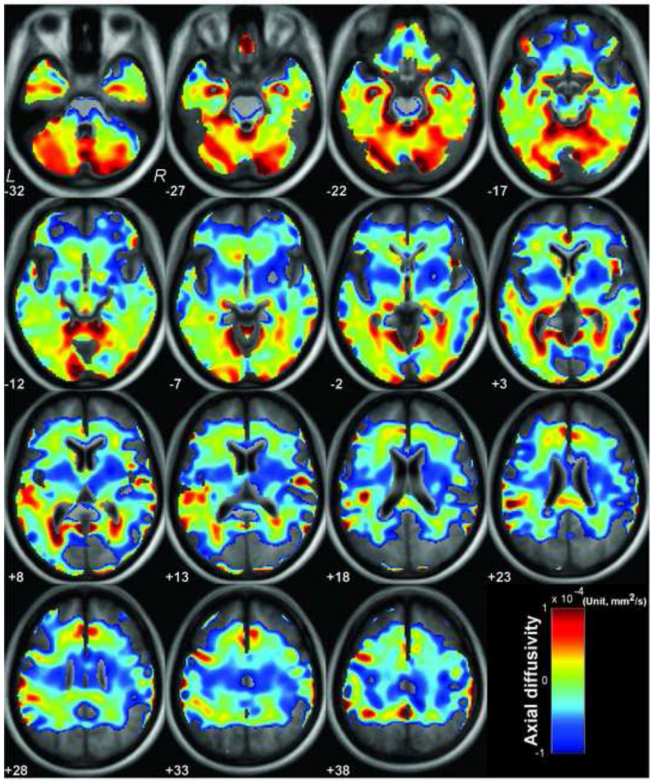

Figure 4.
Whole-brain effect sizes in axial diffusivity between genders. Brain areas with increased and decreased radial diffusivity in males over females are overlaid onto a background image. Other figure conventions are the same as in Figure 2.

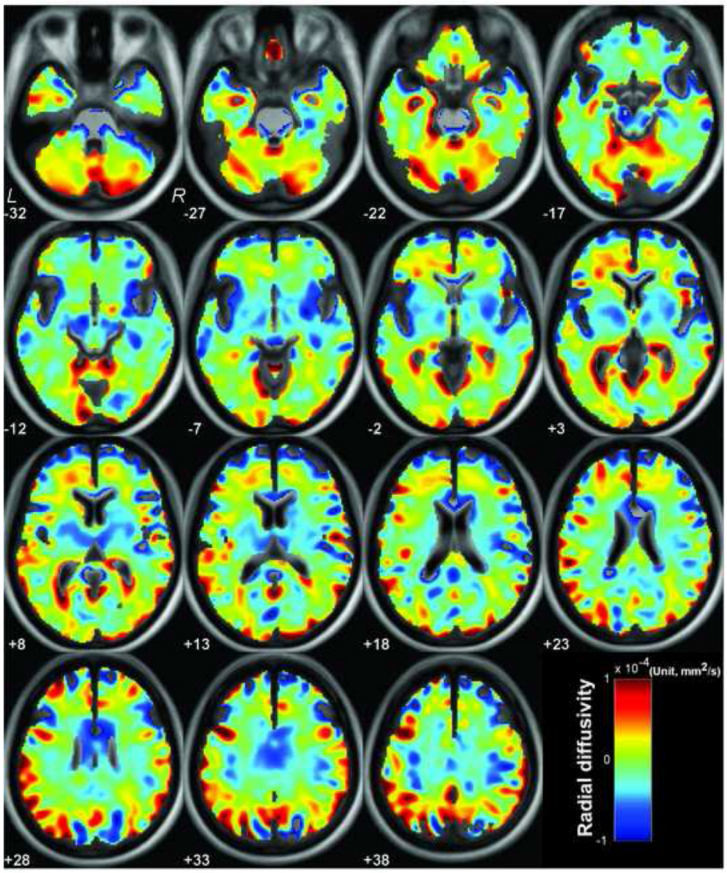

Figure 5.
Whole-brain effect sizes in radial diffusivity between genders. Other figure conventions are the same as in Figure 2.

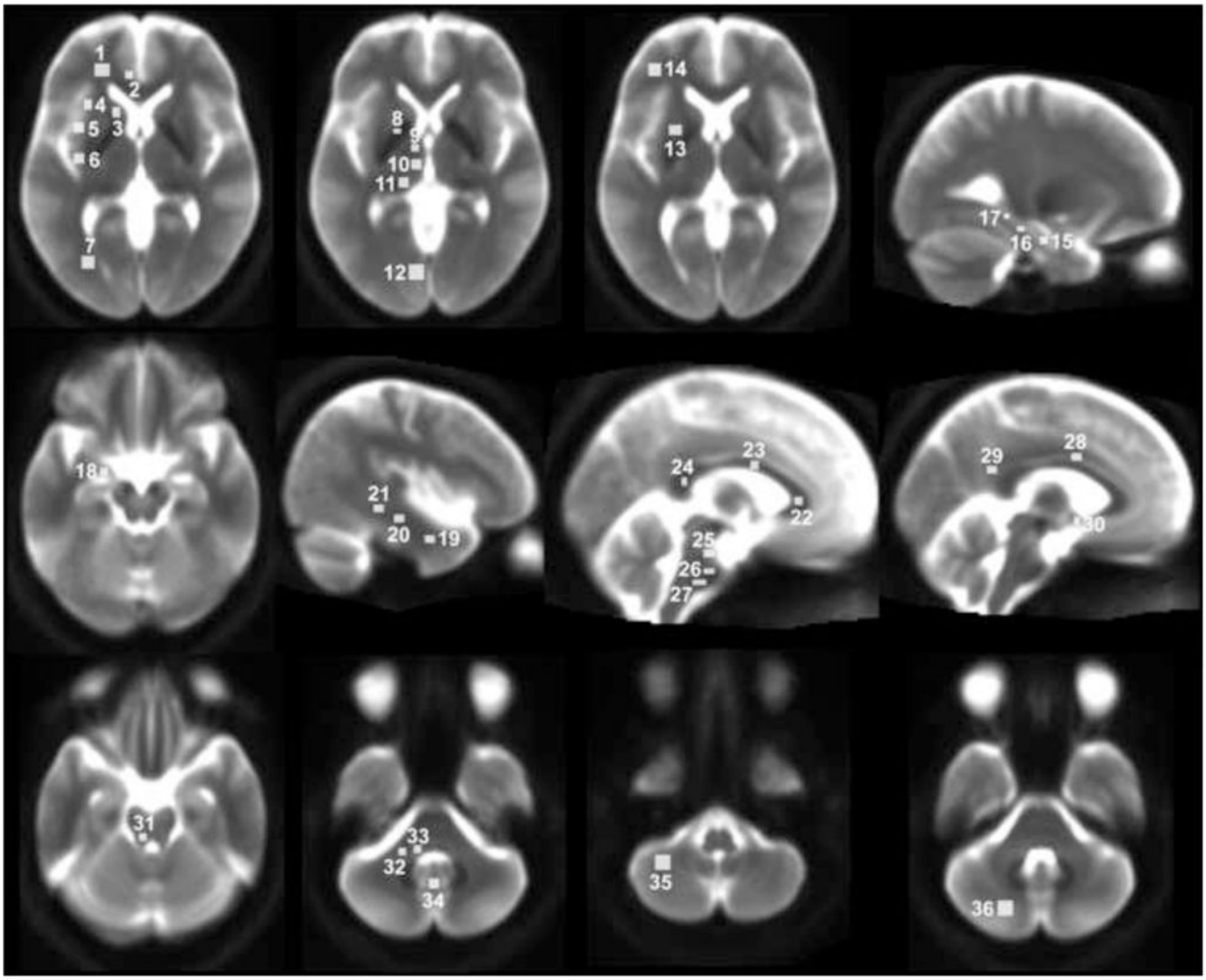

Figure 6.

Regions-of-interest (ROIs) are displayed on mean background images, calculated from normalized and averaged b0 images of all control subjects, and are used to calculate regional axial and radial diffusivity values. ROIs are shown only for the left side on background images for clarity. 1, frontal white matter; 2, anterior cingulate; 3, caudate nucleus; 4, anterior insula; 5, mid insula; 6, posterior insula; 7, occipital white matter; 8, globus pallidus; 9, anterior thalamus; 10, mid thalamus; 11, posterior thalamus; 12, midline occipital gray matter; 13, putamen; 14, frontal gray matter; 15, ventral hippocampus; 16, mid hippocampus; 17, dorsal hippocampus; 18, amygdala; 19, ventral temporal white matter; 20, mid temporal white matter; 21, dorsal temporal white matter; 22, anterior corpus callosum; 23, mid corpus callosum; 24, posterior corpus callosum; 25, caudal pons; 26, mid pons; 27, ventral pons; 28, mid cingulate; 29, posterior cingulate; 30, hypothalamus; 31, superior cerebellar peduncle; 32, mid cerebellar peduncle; 33, inferior cerebellar peduncle; 34 cerebellar deep nuclei; 35, caudal cerebellar cortex; 36, rostral cerebellar cortex.

Brain Res. Author manuscript; available in PMC 2014 May 28.

Table 1

Mean and standard deviation (mean ± SD) axial and radial diffusivity values ($\times 10^{-3}$ mm^2/sec) of brain sites within the rostral area, and male-female differences in those sites.

Brain structures	Axial diffusivity (n = 34)	Axial diffusivity (Male, 19)	Axial diffusivity (Female, 15)	Radial diffusivity (n = 34)	Radial diffusivity (Male, 19)	Radial diffusivity (Female, 15)
L Amygdala *†	1.15±0.13	1.03±0.07	1.21±0.16	0.79±0.10	0.75±0.05	0.83±0.12
R Amygdala *†	1.12±0.12	1.08±0.09	1.17±0.13	0.77±0.08	0.74±0.05	0.81±0.09
L Anterior cingulate	1.18±0.07	1.18±0.07	1.17±0.07	0.76±0.09	0.78±0.09	0.74±0.09
R Anterior cingulate	1.17±0.08	1.16±0.08	1.17±0.07	0.77±0.07	0.78±0.09	0.76±0.05
L Mid cingulate †	1.22±0.06	1.22±0.05	1.22±0.06	0.63±0.06	0.59±0.04	0.67±0.06
R Mid cingulate †	1.23±0.07	1.22±0.08	1.24±0.06	0.63±0.07	0.61±0.06	0.67±0.07
L Posterior cingulate *	1.37±0.20	1.30±0.17	1.46±0.20	0.78±0.09	0.77±0.10	0.80±0.09
R Posterior cingulate *	1.43±0.21	1.36±0.18	1.52±0.21	0.82±0.08	0.80±0.07	0.84±0.09
Anterior corpus callosum	1.58±0.08	1.58±0.07	1.59±0.09	0.51±0.06	0.50±0.05	0.51±0.06
Mid corpus callosum *	1.50±0.15	1.46±0.13	1.56±0.15	0.54±0.08	0.51±0.07	0.57±0.09
Posteror corpus callosum	1.58±0.14	1.60±0.11	1.55±0.16	0.41±0.05	0.42±0.05	0.41±0.04
L Anterior insula	1.20±0.07	1.20±0.06	1.21±0.08	0.81±0.08	0.81±0.08	0.82±0.08
R Anterior insula	1.24±0.11	1.26±0.13	1.22±0.07	0.84±0.10	0.85±0.12	0.81±0.07
L Mid insula	1.31±0.13	1.28±0.13	1.35±0.13	0.94±0.10	0.91±0.10	0.97±0.10
R Mid insula *	1.24±0.10	1.20±0.09	1.28±0.11	0.84±0.08	0.82±0.07	0.87±0.08
L Posterior insula	1.21±0.11	1.18±0.07	1.23±0.15	0.80±0.10	0.78±0.06	0.83±0.13
R Posterior insula	1.20±0.04	1.19±0.04	1.20±0.05	0.74±0.04	0.73±0.03	0.75±0.05
L Caudate nucleus	1.08±0.06	1.07±0.05	1.08±0.07	0.71±0.04	0.70±0.03	0.71±0.05
R Caudate nucleus †	1.08±0.06	1.07±0.05	1.10±0.08	0.71±0.05	0.69±0.04	0.73±0.06
L Frontal gray matter *	1.21±0.11	1.17±0.08	1.26±0.14	0.74±0.09	0.73±0.08	0.75±0.12
R Frontal gray matter	1.16±0.12	1.14±0.09	1.20±0.15	0.71±0.09	0.69±0.07	0.72±0.10
L Frontal white matter †	1.16±0.07	1.16±0.06	1.16±0.07	0.69±0.07	0.71±0.07	0.66±0.06
R Frontal white matter	1.14±0.05	1.13±0.05	1.14±0.06	0.68±0.06	0.69±0.06	0.67±0.06

Brain Res. Author manuscript; available in PMC 2014 May 28.

Brain structures	Axial diffusivity (n = 34)	Axial diffusivity (Male, 19)	Axial diffusivity (Female, 15)	Radial diffusivity (n = 34)	Radial diffusivity (Male, 19)	Radial diffusivity (Female, 15)
L Globus pallidus	1.43±0.14	1.39±0.16	1.48±0.10	0.72±0.11	0.71±0.13	0.74±0.08
R Globus pallidus	1.38±0.15	1.37±0.16	1.39±0.13	0.62±0.12	0.62±0.12	0.61±0.12
L Putamen	1.16±0.08	1.14±0.06	1.19±0.10	0.74±0.05	0.74±0.06	0.75±0.04
R Putamen *†	1.11±0.09	1.07±0.07	1.17±0.09	0.63±0.05	0.62±0.05	0.66±0.05
L Ventral hippocampus	1.22±0.09	1.21±0.10	1.22±0.09	0.86±0.08	0.86±0.08	0.87±0.08
R Ventral hippocampus	1.23±0.10	1.25±0.12	1.20±0.06	0.87±0.06	0.86±0.07	0.87±0.06
L Mid hippocampus	1.11±0.08	1.11±0.08	1.11±0.09	0.72±0.07	0.71±0.06	0.75±0.08
R Mid hippocampus †	1.12±0.06	1.13±0.06	1.12±0.06	0.69±0.06	0.67±0.07	0.71±0.06
L Dorsal hippocampus	1.19±0.24	1.15±0.14	1.25±0.32	0.79±0.11	0.76±0.11	0.82±0.12
R Dorsal hippocampus	1.14±0.11	1.14±0.10	1.15±0.12	0.70±0.07	0.68±0.08	0.72±0.04
L Ventral temporal white matter *	1.29±0.07	1.31±0.08	1.26±0.04	0.73±0.08	0.75±0.09	0.71±0.05
R Ventral temporal white matter	1.18±0.06	1.18±0.05	1.18±0.08	0.63±0.05	0.63±0.05	0.64±0.05
L Mid temporal white matter	1.28±0.06	1.27±0.06	1.29±0.07	0.63±0.05	0.62±0.05	0.64±0.05
R Mid temporal white matter	1.25±0.04	1.25±0.04	1.26±0.04	0.62±0.05	0.61±0.05	0.63±0.06
L Dorsal temporal white matter	1.32±0.06	1.32±0.07	1.32±0.05	0.63±0.07	0.62±0.08	0.63±0.05
R Dorsal temporal white matter	1.30±0.06	1.31±0.05	1.29±0.06	0.64±0.04	0.64±0.05	0.64±0.04
L Mid occipital gray matter	1.26±0.11	1.25±0.08	1.26±0.15	0.85±0.10	0.85±0.11	0.84±0.10
R Mid occipital gray matter	1.22±0.11	1.20±0.07	1.25±0.14	0.78±0.08	0.77±0.06	0.80±0.09
L Occipital white matter	1.17±0.06	1.18±0.06	1.16±0.05	0.65±0.03	0.65±0.03	0.65±0.03
R Occipital white matter	1.13±0.05	1.14±0.04	1.12±0.06	0.65±0.04	0.65±0.04	0.65±0.03

L = Left; R = Right.

*Significant differences in axial diffusivity values between males and females ($p < 0.05$).

†Significant differences in radial diffusivity values between males and females ($p < 0.05$).

Brain Res. Author manuscript; available in PMC 2014 May 28.

Table 2

Mean and standard deviation (mean ± SD) axial and radial diffusivity values ($\times 10^{-3}$ mm^2/sec) of brain regions within the thalamus and hypothalamus, and male female differences in those areas.

Brain structures	Axial diffusivity (n = 34)	Axial diffusivity (Male, 19)	Axial diffusivity (Female, 15)	Radial diffusivity (n = 34)	Radial diffusivity (Male, 19)	Radial Diffusivity (Female, 15)
L Anterior thalalamus *†	1.23±0.08	1.20±0.06	1.28±0.07	0.72±0.07	0.69±0.08	0.75±0.04
R Anterior thalamus *†	1.22±0.06	1.19±0.05	1.25±0.07	0.73±0.06	0.71±0.06	0.77±0.05
L Mid thalamus *†	1.13±0.05	1.11±0.05	1.15±0.05	0.68±0.06	0.66±0.06	0.71±0.04
R Mid thalamus *†	1.15±0.06	1.13±0.05	1.19±0.06	0.68±0.05	0.66±0.06	0.70±0.03
L Posterior thalamus	1.14±0.07	1.15±0.04	1.12±0.10	0.61±0.05	0.60±0.05	0.61±0.04
R Posterior thalamus	1.30±0.09	1.31±0.08	1.29±0.10	0.59±0.04	0.59±0.04	0.58±0.05
L Hypothalamus *†	1.26±0.11	1.22±0.10	1.32±0.10	0.77±0.06	0.75±0.06	0.80±0.05
R Hypothalamus *†	1.25±0.10	1.22±0.09	1.29±0.10	0.78±0.06	0.76±0.05	0.80±0.06

L = Left; R = Right.

*Significant differences in axial diffusivity values between males and females ($p < 0.05$).

†Significant differences in radial diffusivity values between males and females ($p < 0.05$).

Brain Res. Author manuscript; available in PMC 2014 May 28.

Table 3

Mean and standard deviation (mean ± SD) axial and radial diffusivity values ($\times 10^{-3}$ mm^2/sec) of brain sites within the cerebellum and pons areas, and male-female differences.

Brain structures	Axial diffusivity (n = 34)	Axial diffusivity (Male, 19)	Axial diffusivity (Female, 15)	Radial diffusivity (n = 34)	Radial diffusivity (Male, 19)	Radial diffusivity (Female, 15)
Caudal pons *†	1.66±0.44	1.49±0.41	1.86±0.40	0.94±0.34	0.81±0.34	1.12±0.32
Mid pons †	1.26±0.32	1.16±0.13	1.38±0.44	0.61±0.25	0.52±0.09	0.72±0.33
Ventral pons †	1.09±0.06	1.18±0.06	1.20±0.05	0.55±0.07	0.52±0.07	0.58±0.06
L Caudal cerebellar cortex *	1.00±0.06	1.03±0.06	0.97±0.04	0.63±0.05	0.64±0.05	0.62±0.04
R Caudal cerebellar cortex †	1.05±0.07	1.07±0.08	1.02±0.04	0.66±0.07	0.68±0.07	0.63±0.05
L Rostral cerebellar cortex	1.00±0.05	1.00±0.06	1.01±0.04	0.61±0.04	0.60±0.04	0.61±0.05
R Rostral cerebellar cortex	1.04±0.08	1.04±0.09	1.04±0.04	0.63±0.06	0.62±0.06	0.64±0.05
Cerebeller deep nuclei *	1.06±0.06	1.08±0.05	1.03±0.06	0.64±0.04	0.65±0.04	0.64±0.04
L Inferior cerebellar peduncle	1.19±0.09	1.20±0.09	1.17±0.09	0.64±0.06	0.64±0.07	0.64±0.06
R Inferior cerebellar peduncle *†	1.16±0.08	1.14±0.05	1.20±0.09	0.60±0.07	0.57±0.05	0.64±0.06
L Middle cerebellar peduncle *	1.16±0.05	1.18±0.05	1.14±0.05	0.48±0.03	0.47±0.03	0.48±0.03
R Middle cerebellar peduncle	1.19±0.05	1.20±0.05	1.19±0.06	0.47±0.04	0.46±0.05	0.48±0.03
L Superior cerebellar peduncle †	1.28±0.06	1.27±0.06	1.30±0.07	0.52±0.05	0.50±0.05	0.55±0.05
R Superior cerebellar peduncle †	1.32±0.11	1.31±0.07	1.35±0.15	0.54±0.10	0.50±0.07	0.59±0.12

L = Left; R = Right.

*Significant differences in axial diffusivity values between males and females ($p < 0.05$).

†Significant differences in radial diffusivity values between males and females ($p < 0.05$).